Negative Knudsen force on heated microbeams

Taishan Zhu,[1] Wenjing Ye,[1,2,*] and Jun Zhang[1,3]
[1]*Department of Mechanical Engineering, The Hong Kong University of Science and Technology, Hong Kong*
[2]*KAUST-HKUST Micro/Nanofluidic Joint Laboratory, The Hong Kong University of Science and Technology, Hong Kong*
[3]*Laboratory of High Temperature Gas Dynamics, Institute of Mechanics, Chinese Academy of Sciences, Beijing, People's Republic of China*
(Received 6 July 2011; revised manuscript received 4 October 2011; published 18 November 2011)

Knudsen force acting on a heated microbeam adjacent to a cold substrate in a rarefied gas is a mechanical force created by unbalanced thermal gradients. The measured force has its direction pointing towards the side with a lower thermal gradient and its magnitude vanishes in both continuum and free-molecule limits. In our previous study, negative Knudsen forces were discovered at the high Knudsen regime before diminishing in the free-molecule limit. Such a phenomenon was, however, neither observed in experiment [A. Passian *et al*., Phys. Rev. Lett. **90**, 124503 (2003)], nor captured in the latest numerical study [J. Nabeth *et al*., Phys. Rev. E **83**, 066306 (2011)]. In this paper, the existence of such a negative Knudsen force is further confirmed using both numerical simulation and theoretical analysis. The asymptotic order of the Knudsen force near the collisionless limit is analyzed and the analytical expression of its leading term is provided, from which approaches for the enhancement of negative Knudsen forces are proposed. The discovered phenomenon could find its applications in novel mechanisms for pressure sensing and actuation.

DOI: 10.1103/PhysRevE.84.056316 PACS number(s): 47.61.−k, 47.45.Dt, 51.10.+y, 51.90.+r

I. INTRODUCTION

Thermal force created by thermal inhomogeneity in nonequilibrium systems has fascinated scientists since the 19th century. As a unique actuation mechanism, mechanical forces can be created devoid of moving parts and physical contact. The early successful application of such an actuation mechanism was made by Crookes in 1873, who devised the famous radiometer, also known as the light mill [1]. The reason for the rotation, however, was not clear at the time and has been the cause of a long-standing scientific debate. It was not until recently that an experimental and numerical analysis was carried out and the origin of the rotation was identified [2]. Another well-known phenomenon induced by this type of force is thermophoresis, in which a small particle migrates in a gas under the influence of the thermophoretic force stemming from temperature gradients. Since its discovery in 1870 [3], voluminous work has been devoted to the study of the mechanism of this force and to evaluating its magnitude either analytically or numerically [4–9]. On the basis of the Boltzmann equation, asymptotic analyses [6,9] suggested that, near the continuum regime, thermal creep flow is the dominant driving mechanism that causes the thermophoretic force when the temperature of the particle is nonuniform. As a result, the magnitude of the force is of $O(\mathrm{Kn}^2)$ with Kn, the Knudsen number defined as the ratio of molecular mean free path and particle characteristic length. When the particle's thermal conductivity is much larger than that of the surrounding gas, its temperature is nearly uniform and thermal stress slip flow dominates, producing a force of $O(\mathrm{Kn}^3)$ [9]. It was also found that the force in this case reversed its direction to that of the temperature gradient. However, due to the lack of experimental support, it was argued in Ref. [10] that the negative thermophoresis could be an artifact due to the models of the Boltzmann equation. Although there is no experimental evidence of the "negative thermophoresis," such a phenomenon was nevertheless noted by several researchers using different theoretical approaches [11,12].

With the advent of microfabrication techniques, micro and nano devices with integrated heaters have been routinely made and employed for various applications, such as pressure and topographic sensing [13–15]. The small scale of the devices and the large thermal gradient provide two necessary conditions for the thermal force to be present, which may benefit or deteriorate the performance of the devices. Recently Passian *et al*. have demonstrated a mechanical force, entitled as the Knudsen force, acting on a heated micromachined cantilever embedded in a cold vacuum chamber [16]. The experimental results have shown that this force is proportional to the ambient pressure in the low-pressure range, but inversely proportional to pressure in the high-pressure range.

A direct simulation Monte Carlo (DSMC) study based on the assumption of fully diffuse surfaces was conducted to investigate the origin of the Knudsen force [17]. It was found that flow induced by the corners of the cantilever is the main driving mechanism. Equally intriguing is the newly discovered phenomenon from the simulations that, similar to the negative thermophoresis, the Knudsen force also demonstrates the capability of changing its direction. At high-Kn situations before it vanishes in the collisionless limit, the direction of the force points towards the region with higher thermal gradient, pushing the cantilever towards the substrate. Such a phenomenon has never been reported elsewhere and was not observed in the experiment of Passian *et al*. [16] as well as in the numerical analysis of the same problem based on the Boltzmann equation with the ellipsoidal statistical Bhatnagar-Gross-Krook model (Nabeth *et al*. [18]).

A qualitative discussion was provided in Ref. [18] on the direction of the Knudsen force. It was argued that, even though the net impulse is given to the beam from two molecules colliding with the beam from upper and lower points downwards, the number of molecules hitting the beam from the top is less than those hitting the beam from the bottom due

*mewye@ust.hk

to the thermally induced vortices, resulting in an upward net force. However, this argument is sound when the top vortex is strong. At high Knudsen numbers, particularly near the collisionless limit, thermally induced flow which vanishes in the collisionless limit is very weak and may not be able to effectively block the top molecules from hitting the beam. In this paper, we use gas kinetic theory to theoretically justify the existence of the negative Knudsen force at high Knudsen numbers. We also analyze the order of the force near the collisionless limit and propose methods for the enhancement of such negative forces.

II. DSMC SIMULATION

We consider a two-dimensional (2D) model problem as depicted in Fig. 1. A hot rectangle representing the cross section of a heated microbeam is embedded inside a larger rectangle signifying the vacuum chamber. The temperatures of the microbeam and chamber are T_b and T_a ($T_a < T_b$), respectively. The width and height of the beam and chamber are denoted by l, h, and L, H. This beam is placed closer to the bottom wall so that $G > g$, G and g being the distances from the beam to the top and the bottom chamber walls. We first consider a domain with $l = 10$ μm, $h = 2$ μm, $L = 20$ μm, $H = 8$ μm, and $g = 1$ μm. In addition to the cases with argon ambient gas simulated in our previous study [17], two more cases with helium and nitrogen are simulated. In these simulations, temperatures are set to be $T_a = 300$ K, $T_b = 500$ K. A diffuse boundary is assumed for all solid surfaces. A variable hard sphere model is employed for all gases. For nitrogen, energy transfer between internal modes is modeled using the Larsen-Borgnakke model [19]. Other parameters such as cell size, time step, etc., are the same as those employed in Ref. [17]. The description of the DSMC method and the formula for the calculation of the Knudsen force can also be found therein.

Figure 2 plots the calculated Knudsen forces per unit length corresponding to three different ambient gases as functions of the initial chamber pressure, which is determined from a given initial number density n_0 and a reference temperature of 273 K. Logscale is employed for pressure here for a clear illustration

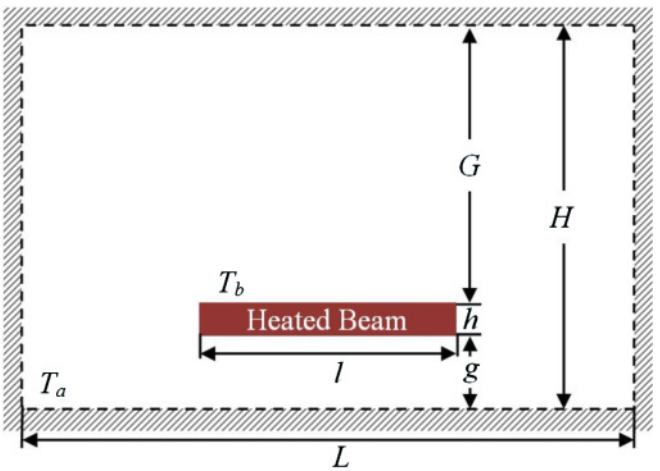

FIG. 1. (Color online) Schematic illustration of the 2D problem domain. T_b represents the temperature of the beam; T_a denotes the temperature of the chamber wall. In this work, it is set to be uniform.

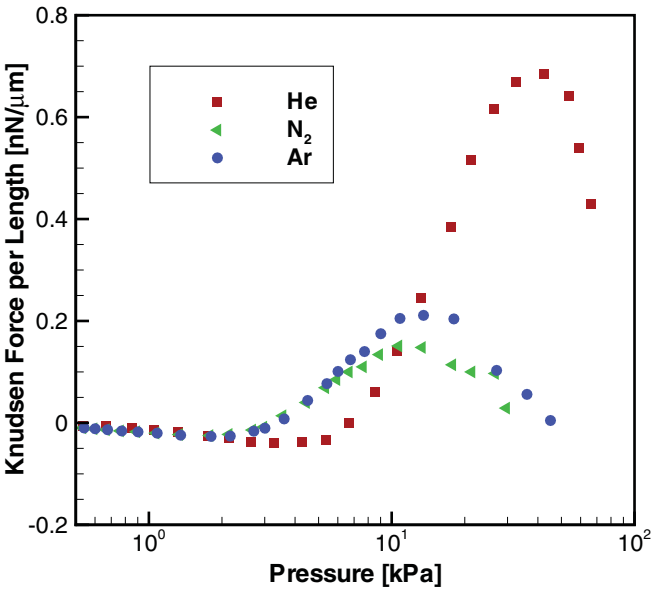

FIG. 2. (Color online) Computed Knudsen forces corresponding to three different ambient gases.

of the negative forces. Except for the region where the Knudsen force becomes negative, the qualitative trends of three curves are consistent with the experimental data of Passian *et al.* [16]. All curves peak in the range between 10 and 50 kPa which is in the early transition regime. Similar to the experimental results, the peak location and its magnitude vary with gas species with the force corresponding to helium being the largest.

Figure 3 shows the normalized force against the Knudsen number defined as $\mathrm{Kn} = \lambda/g$, where the mean-free path λ is based on the average temperature $T_{\mathrm{avg}} = (T_a + T_b)/2$. The nominal force is calculated based on the average of the gas pressure determined by $P = n_0 k T_{\mathrm{avg}}$. The existence of

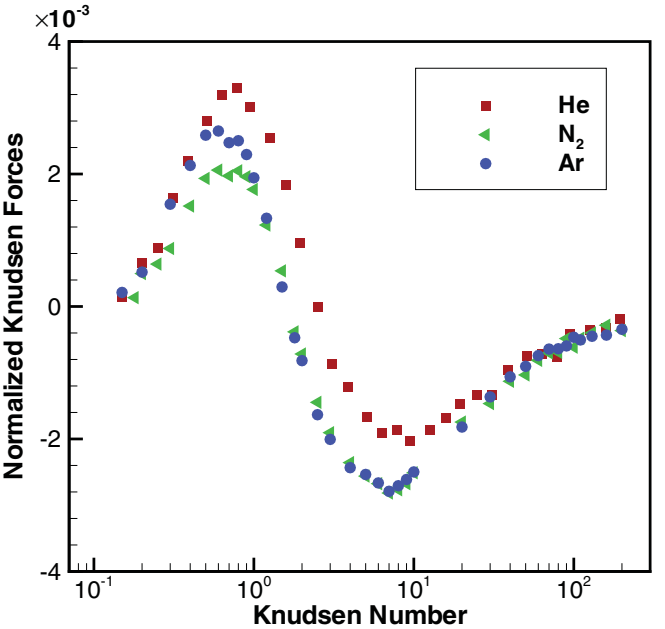

FIG. 3. (Color online) Normalized Knudsen forces as functions of Knudsen number.

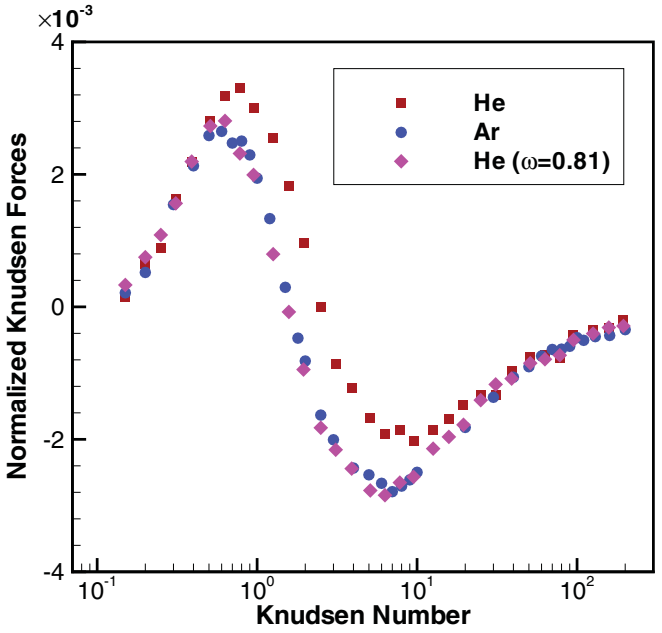

FIG. 4. (Color online) Comparison of normalized Knudsen forces for monatomic gases with different temperature exponents of the coefficient of viscosity.

the negative forces is evident in this figure. In all cases, the normalized force reverses its direction near Kn = 2 and reaches its maximum negative value at Kn ∈ (5,10). Moreover, despite the same geometrical dimensions and structure temperatures, these three curves do not collapse into one, particularly in the low- and medium-Kn regimes. Such a fact suggests that intermolecular collisions play an important role in the Knudsen force. It has been found that the heat capacity ratio γ and the temperature exponent of the coefficient of viscosity ω are the two parameters that contribute to the differences. For monatomic gases, if temperature dependence of the coefficient of viscosity is assumed to be the same for all gases, dimensional analysis indicates that force curves should collapse into a single one since they have the same γ. This indeed can be observed in Fig. 4 in which normalized forces per length obtained for helium with its ω set to be the same as that of argon are also plotted. It should be pointed out that diffuse walls are assumed for all cases in this study. In Ref. [18] it was found that forces calculated with a smaller accommodation coefficient fit better with the experimental results for helium.

The results presented in Figs. 2 and 3 are obtained for the temperature difference of 200 K which is an order of magnitude larger than the temperature difference in the experiment of Passian *et al.*. To investigate the influence of the temperature difference on the negative Knudsen force, a domain closer to the experimental setup is considered here. The dimensions of the beam and the chamber are set to be $l = 10\ \mu$m, $h = 1\ \mu$m and $L = 20\ \mu$m, $H = 7\ \mu$m, such that the gap g and the ratio g/G remain unchanged. The temperatures are set to be $T_a =$ 300 K and $T_b = 330$ K, which yields a temperature difference of 30 K. DSMC simulations were conducted for argon. The number of samples and the number of simulation particles are chosen such that the fractional error of the calculated pressure is of the order 10^{-5}. The computed Knudsen forces at two Knudsen numbers together with the corresponding values of the previous case are listed in Table I. Again, negative Knudsen forces at high Knudsen numbers are predicted. The magnitude of the forces is, however, much smaller than that in the case with a 200 K temperature difference. Such small forces would be very hard to detect experimentally which may explain their absence in the measurements.

TABLE I. Knudsen forces in two cases.

	Knudsen forces (nN/μm)	
Kn	Case I	Case II
	$\Delta T = 200$ K	$\Delta T = 30$ K
5	−0.02	−0.0032
40	−0.001 04	−0.000 14

III. GAS-KINETIC ANALYSIS: NEAR THE COLLISIONLESS LIMIT

It is well recognized that a nonuniform temperature distribution inside a gas induces a nonuniform pressure profile when the gas is rarefied. In the collisionless limit, Knudsen proved that $PT^{-1/2}$ remains constant inside a closed system at the steady state [20]. This conclusion was drawn based on the assumption that the density function of molecular velocities follows the Maxwell distribution. Wu revised the theory and proposed to use an isotropic factor,

$$I(\mathbf{x}) = 4\pi\left[\int_{\varphi=0}^{\pi}\int_{\theta=0}^{2\pi}(T_{\varphi\theta})^{1/2}\sin\varphi d\varphi d\theta \times \int_{\varphi=0}^{\pi}\int_{\theta=0}^{2\pi}(T_{\varphi\theta})^{-1/2}\sin\varphi d\varphi d\theta\right]^{-1/2},$$

where $T_{\varphi\theta}$ is the temperature at $\mathbf{x}$ defined in a spherical coordinate system, to account for any anisotropic distribution [21]. He proved that, instead of $PT^{-1/2}$, $PT^{-1/2}I$ should be the invariant and the conclusion is valid for any temperature distribution with arbitrary thermal accommodation coefficients on the boundary of a closed system in the collisionless limit. Based on Wu's theory, one expects that at very high Knudsen numbers when intermolecular collisions are negligible, $PT^{-1/2}I$ remains constant throughout the problem domain. To estimate the Knudsen range in which this conclusion holds, we check the variation of $PT^{-1/2}I$ defined as $\Delta\xi = (\xi_{\max} - \xi_{\min})/\xi_{\min}$, where $\xi = PT^{-1/2}I$, in our problem using DSMC simulations and plot it in Fig. 5. For a tolerance of 1%, $\xi = PT^{-1/2}I$ can be regarded as a constant when the Knudsen number is larger than 30.

Consider two points A and B, distinguished by subscript t and b, located on the same vertical line with A being on the top surface and B being on the bottom surface of the cantilever. The invariant allows us to express the normalized pressure difference at the two points as

$$f = \frac{P_b - P_t}{P_0} = \left(\frac{T_b}{T_0}\right)^{1/2}\frac{I_0}{I_b} - \left(\frac{T_t}{T_0}\right)^{1/2}\frac{I_0}{I_t}, \qquad (1)$$

where P_0, T_0, and I_0 are the pressure, temperature, and isotropic factor at the reference state. It is obvious for our

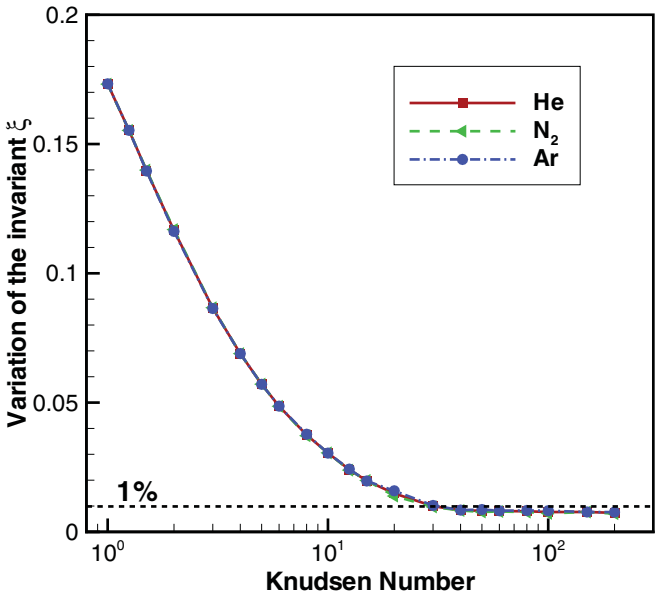

FIG. 5. (Color online) Variations of $PT^{-1/2}I$ at different Knudsen numbers.

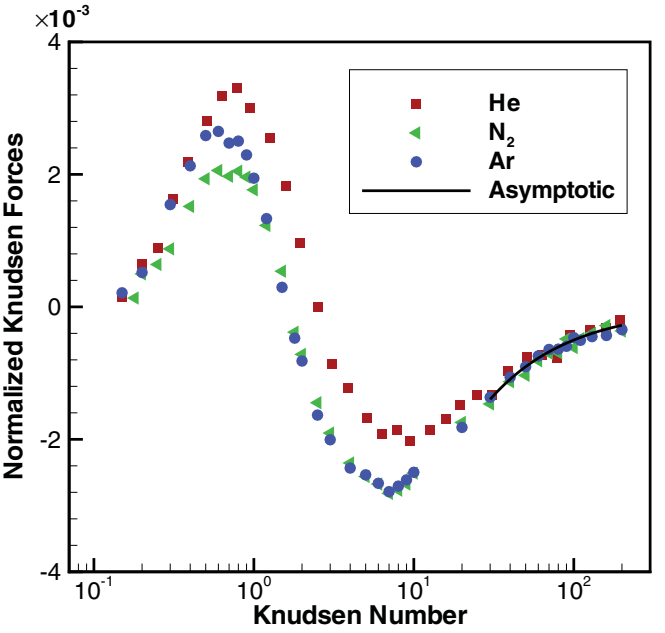

FIG. 6. (Color online) Normalized Knudsen forces versus Knudsen number.

cases that $I_b = I_t = I$ because both chamber and cantilever are isothermal and diffuse boundary is assumed for all surfaces. This fact leads to the following expression for the normalized pressure difference:

$$f = \frac{I_0}{I}\left[\left(\frac{T_b}{T_0}\right)^{1/2} - \left(\frac{T_t}{T_0}\right)^{1/2}\right]. \tag{2}$$

From Eq. (2) we first notice that, because $T_b < T_t$, the direction of net pressure should point downwards which is opposite to the direction of the force when the Knudsen number is small. We also realize that as Kn decreases, the magnitude of the negative Knudsen force increases due to the growing temperature difference. To identify its order, we expand the temperatures at the two points around the collisionless limit T_f,

$$\frac{T_b - T_f}{T_f} = a_1 \mathrm{Kn}_b^{-1} + a_2 \mathrm{Kn}_b^{-2} + \cdots, \tag{3}$$

$$\frac{T_t - T_f}{T_f} = b_1 \mathrm{Kn}_t^{-1} + b_2 \mathrm{Kn}_t^{-2} + \cdots, \tag{4}$$

where Kn_b and Kn_t are the local Knudsen numbers at points B and A. Taking the leading term only, we have

$$T_b^{1/2} - T_t^{1/2} = \tfrac{1}{2} T_f^{1/2}\left(a_1 \mathrm{Kn}_b^{-1} - b_1 \mathrm{Kn}_t^{-1}\right). \tag{5}$$

The local Knudsen numbers Kn_b and Kn_t are related by $\mathrm{Kn}_t = \frac{g}{G}\mathrm{Kn}_b$. In addition, the force vanishes when the beam is at the center of the chamber, that is, $g = G$. Hence the normalized pressure difference becomes

$$f = \frac{1}{2}\frac{I_0}{I}\left(\frac{T_f}{T_o}\right)^{1/2} a_1 \left(1 - \frac{g}{G}\right)\mathrm{Kn}_b^{-1}. \tag{6}$$

It is evident from Eq. (6) that the pressure difference near the collisionless limit is caused by the unbalanced thermal gradient in the vertical direction. Hence the pressure difference in the vertical direction likely contributes the most to the Knudsen force. Based on our DSMC simulations, among the three normal pressure components P_{xx}, P_{yy}, and P_{zz}, the difference in P_{yy} at the two points A and B indeed contributes the most to f. For example, in the case with 30 K temperature difference, at $\mathrm{Kn} = 40$, the average ΔP_{xx} of the top and the bottom surfaces of the beam is five times smaller than the average ΔP_{yy}. Moreover ΔP_{xx} decays much fast than ΔP_{yy} as Kn increases. The force coming from the shear stress P_{xy} acting along the thickness of the beam, which also points downwards, is about one order of magnitude less than the force resulting from ΔP_{yy}. Hence the net force acting on the beam is of $O(\mathrm{Kn}_b^{-1})$ and is along the negative y direction. To demonstrate its order, a function of the form $f = c(1 - \frac{g}{G})\mathrm{Kn}^b$ is employed

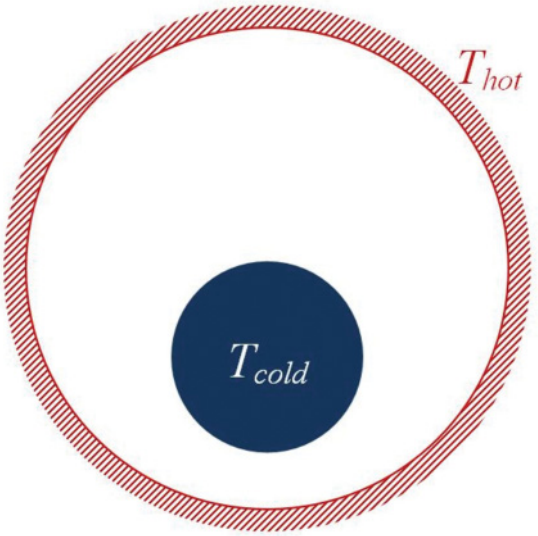

FIG. 7. (Color online) Schematic of the problem of Aoki *et al.* [22].

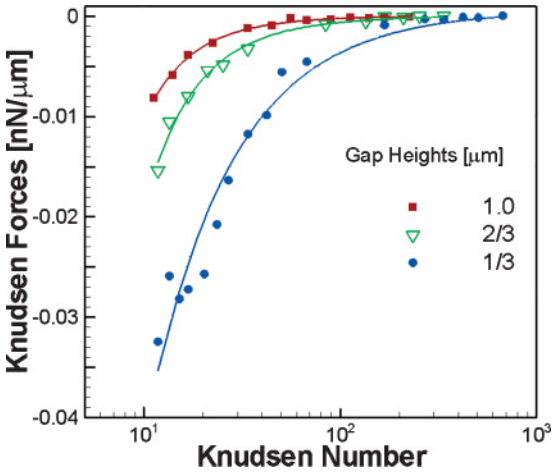

FIG. 8. (Color online) Negative Knudsen forces at different gap heights.

to fit the DSMC data corresponding to Kn $\in$ (30, 200). The coefficients c and b are found to be around –31.56 and –0.85. The agreement between the analytical form and DSMC simulation is quite good as depicted in Fig. 6.

Similar analysis can also be applied to the Knudsen force on a heated circular cylinder embedded in a cold cylindrical chamber (see Fig. 7). Based on the analysis, the Knudsen force should point towards the positive y direction in the near-collisionless regime since the temperature at the lower surface of the inner cylinder is higher than the temperature at the upper surface of the inner cylinder. Aoki *et al*. performed a numerical analysis of this problem on the basis of the linearized Boltzmann-Krook-Welander equation in the entire Kn range [22]. The simulated Knudsen force at high Knudsen numbers is along the positive y-direction which is consistent with the direction predicted by our theoretical analysis.

The negative Knudsen force, although it exists, has a very small magnitude compared to the positive force at small Knudsen numbers. Unless its magnitude is enhanced, such a force would be very difficult to detect, let alone be of any practical use. The theoretical analysis, Eq. (6), indicates that in addition to the temperature difference, the ratio of the two gaps, g/G, is a key parameter that determines the magnitude of the negative Knudsen force. A smaller ratio would increase the magnitude of the force. DSMC simulations are conducted for argon with $g = 1/3$ μm and $g = 2/3$ μm. All other dimensions remain the same as those in case 1; that is, the temperature difference between the microbeam and chamber is 200 K. The simulated Knudsen forces are plotted in Fig. 8. Solid lines are obtained via curve fitting. As expected, the magnitude of the negative Knudsen force increases with the decreasing g/G.

IV. CONCLUSIONS

Negative Knudsen forces have been discovered from the numerical modeling of a heated microbeam next to a cold wall using the direction simulation Monte Carlo method. It has been found that the Knudsen force switches its direction in the transition regime and maintains its "negative" orientation before it diminishes in the collisionless limit. However, the magnitude of negative forces turns out to be very small compared to that of the positive counterparts at small Knudsen numbers. For a temperature difference of 200 K, a g/G ratio of 0.2, and argon ambience, the maximum negative force is about one order smaller than the maximum positive force. Such a small magnitude might well be the reason that causes its absence in the experiment of Passian *et al*.

An analytical analysis has been conducted to further confirm the existence of such a negative force and to identify its asymptotic order near the collisionless limit. It has been found that the negative Knudsen force is of $O(\mathrm{Kn}_b^{-1})$ and its magnitude depends also on the ratio of g/G in addition to temperature difference. One approach to boost its magnitude without increasing the temperature difference is to increase this ratio. A numerical simulation has been performed to demonstrate the feasibility of this approach.

ACKNOWLEDGMENTS

This work is supported in part by Award No. SA-C0040/UK-C0016, made by King Abdullah University of Science and Technology, and in part by Hong Kong Research Grants Council under Competitive Earmarked Research Grant No. 621408.

[1] W. Crooks, Philos. Trans. R. Soc. London **163**, 277 (1873).
[2] N. Selden C. Naglande, S. Gimelshein, E. P. Muntz, A. Alexeenko, and A. Ketsdever, Phys. Rev. E **79**, 041201 (2009).
[3] J. Tyndall, Proc. R. Inst. **6**, 1 (1870).
[4] P. S. Epstein, Z. Phys. **54**, 537 (1929).
[5] J. R. Brock, J. Colloid Sci. **17**, 768 (1962).
[6] Y. Sone and K. Aoki, Prog. Astronaut. Aeronaut. **51**, 417 (1977).
[7] L. Waldmann, Z. Naturforsch. **14**, 589 (1959).
[8] Y. Sone and K. Aoki, J. Mec. Theor. Appl. **2**, 3 (1983).
[9] T. Ohwada and Y. Sone, Eur. J. Mech., B: Fluids **11**, 389 (1992).
[10] F. Zheng, Adv. Colloid Interface Sci. **97**, 255 (2002).
[11] H. A. Dwyer, Phys. Fluids **10**, 977 (1967).
[12] S. Beresnev and V. Chernyak, Phys. Fluids **7**, 1743 (1995).
[13] C. H. Mastrangelo and R. S. Muller, IEEE J. Solid-State Circuits **26**, 1998 (1991).
[14] P. K. Weng and J. S. Shie, Rev. Sci. Instrum. **65**, 492 (1994).
[15] W. P. King, T. W. Kenny, and K. E. Goodson, Appl. Phys. Lett. **85**, 2086 (2004).
[16] A. Passian, R. J. Warmack, T. L. Ferrell, and T. Thundat, Phys. Rev. Lett. **90**, 124503 (2003).
[17] T. Zhu and W. Ye, Phys. Rev. E **82**, 036308 (2010).
[18] J. Nabeth, S. Chigullapalli, and A. Alexeenko, Phys. Rev. E **83**, 066306 (2011).
[19] C. Borgnakke and P. Larsen, J. Comput. Phys. **18**, 405 (1975).
[20] M. Knudsen, Ann. Phys. **31**, 205 (1910); **31**, 633 (1910); **34**, 593 (1911).
[21] Y. Wu, J. Chem. Phys. **48**, 889 (1968).
[22] K. Aoki, Y. Sone, and T. Yano, Phys. Fluids A **1**, 409 (1989).